January 1991

Critical Phenomena from diamagnetic signal in high Tc perovskites

Juana Acrivos
San José State University

M. Chen Lei
San Jose State University

B168.10

Critical phenomena from diamagnetic signal in high T_c perovskites

J.V. Acrivos and M. Chen Lei, San Jose State University San Jose Ca 95192-0101

Abstract. Critical phenomena in nearly two-dimensional high T_c superconductors are detected by induction measurements of the shielding current produced by bulk quantization of flux vs H_z.

1. Introduction.

The high T_c superconductors are of type II and in fields $H > H_{c1} \approx .05$ Oe, the enhancement of the diamagnetism as $T \to T_c$ is used to determine the transition temperature which is also detected by the discontinuity in the heat capacity as measured by differential calorimetry.

2. Experimental.

The sample (Figure 1) preparation and signal detection at $\nu = 8$ MHz, field modulation $H_{mz} = 2H_m \sin 2\pi\nu_m t$ when $H_m < 0.05$ Oe are described elsewhere.[1] The magnitude of the induced diamagnetic signal vs $H_z = 0 \pm 5$ Oe is measured in a resonant rf circuit as a function of time as the temperature T goes from 77 K past T_c as defined by the heat capacity C_p. Figure 2 shows the temperature change vs time t and, as $T \to T_c$, $dT/dt = \delta q/C_p \to 0$, when δq is the constant heat absorbed per unit t. Samples (Fig. 1) are made of 10 µm lamellae dispersed in 5 min. epoxy and cured in a magnetic field of 9 T. The diamagnetic signal is enhanced as $T \to T_c$ in Fig. 2. The field and the susceptibility were calibrated by low field esr.[2]

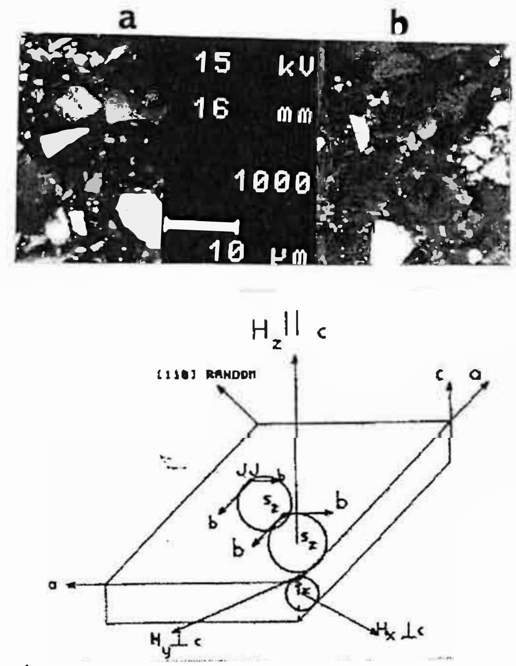

Fig. 1 Sample: SEM of aligned lamellae. a: $Y_1Ba_2Cu_3O_7$, b: $Tl_{.3}Ca_2Ba_2Cu_2O_x$, and. c: Sample in laboratory axes.

3. Results.

The diamagnetism in a superconductor behaves as:[3]

$$= -10^{-7} * |T_c/(T_c-T)|^{\frac{1}{2}}, \quad (1)$$

and here T_c is determined by $dT/dt \to 0$. The anisotropy in the diamagnetic signal S vs $\alpha = H_z \hat{} H_0$ (when $H_0 \|$ c-axis, in Fig. 1) was measured with the rf field $2H_1 \sin 2\pi\nu t$ both normal and parallel to the external field H_z. The orientation dependence shown in Fig. 3 indicates that S is a maximum for $c \|$ $B = k\, H_z + H_{mz} + 2\, i/k\, H_1 \sin 2\pi\nu t$.

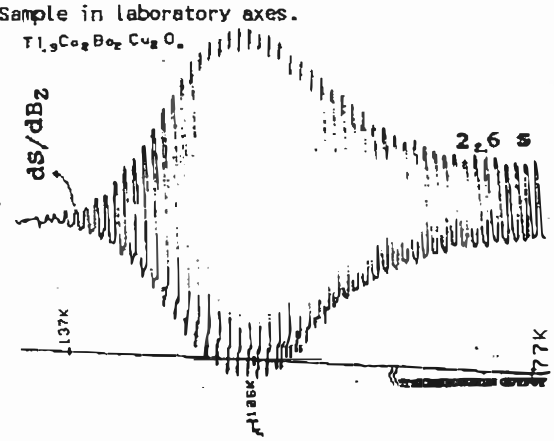

Fig. 2 Meissner Signal vs T. $\nu_m = 400$ Hz. H_z is swept every 2.6 s about ± 5 Oe. T is measured by a Cu-constantan thermocouple.

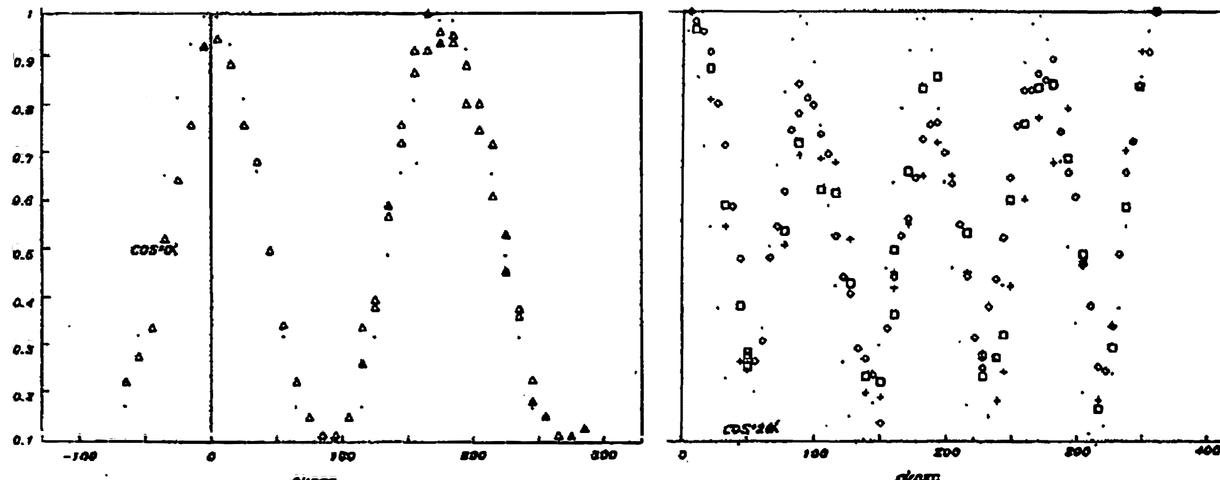

Fig.3 Orientation dependence of Meissner Signal: $a{:}H_1||H_z\perp H_y$. $b{:}H_1\perp H_z\perp H_y$.
The dots give the calculated functions $a{:}\cos^2\alpha$, $b{:}\cos^2 2\alpha$. The data points are for different runs.

4. Discussion.

The intercepted flux in a field B is in units of $\Phi_0=h/2e$:[4a]

$$f_m\equiv \Phi_m/\Phi_0 = f_e + Li(circ)/\Phi_0 = m, \qquad (2)$$

for a perfect superconducting cylinder. $f_e \equiv \mathbf{B}.\mathbf{n}_0 O/\Phi_0$, $\mathbf{n}_0$ is the outward unit normal to the enclosed area O and L is the self inductance of the superconducting loop *1* in Figure 1. In a singly connected superconductor m changes by ±1 at $f_e=(m \pm \frac{1}{2})$ and i(circ) changes discontinuously giving rise to a a saw tooth current vs the external flux. When there is a Josephson junction in the path of the current loop, $i(circ) = i_c \sin\triangle\phi$ (where i_c is the critical current) is the tunnel current and the change in phase angle required for the continuity of the wave function is $\triangle\phi = 2\pi(m-f_m)/N$. Then f_m becomes:[4a,b]

$$f_m= f_e - f_s \sin(2\pi(f_m - m)/N), \qquad (3)$$

$f_s = Li_c/\Phi_0$ and the contributions to the inductance must include the Josephson inductance, $L_J i_c/\Phi_0 \cos\triangle\phi = 1/2\pi$,[5] and that in the loop of radius r ($L = 4\pi 10^{-7} r \ln(r/a) \approx 3{*}10^{-12}$ H when $r\approx 1$ µm and $a\approx 0.1$ µm) and, the contribution from the self inductance is of the same order as that from the Josephson inductance only if the current density is $\approx 10^6$ A/cm². The system makes the transition $\triangle m=\pm 1$ when i(circ) reaches the value $\pm i_c$.[4]

The induced emf in units of Φ_0/t is:[4a]

$$-df_m/dt=-[df_e/dt]/[1+2\pi f_s/N\cos\triangle\phi], \qquad (4)$$

$$df_e/dt=2[H_m w_m s_z \cos(w_m t)+H_1 w s_x \cos(wt)]/\Phi_0$$

and both H_1 and H_m are determined by H_{c1}. Other important sample parameters are s_z the area enclosing i(circ) normal to H_z, and s_x, that normal to H_x in Fig. 1. The periodicity $\triangle H_z$ is determined in Fig. 4 when $\triangle f_e = \triangle H_z\, \Sigma s_z/\Phi_0 = 1$ and depends on the parameters N and f_s. In the laboratory axes shown in Fig. 1 $H_z||c$ and, the s_z are in the **a**,**b** plane while s_x is in a plane normal to **a**,**b** with projections on the (110) and/or (1$\bar{1}$0) planes. A distribution of $O\approx\Sigma s_z$ and of f_s about an average gives rise to a line width $\triangle H_{ms}$ = 50µT. The energy stored in the loop *1* is given by:[4]

$$E = 1/2\ Li^2 - N\Phi_0 i_c/2\pi \cos\triangle\phi + K, \qquad (5)$$

where K is a constant and, as $f_m \rightarrow m$:

$$E = A\ (f_m - m)^2 - 2|V|^2/A + K \qquad (6)$$

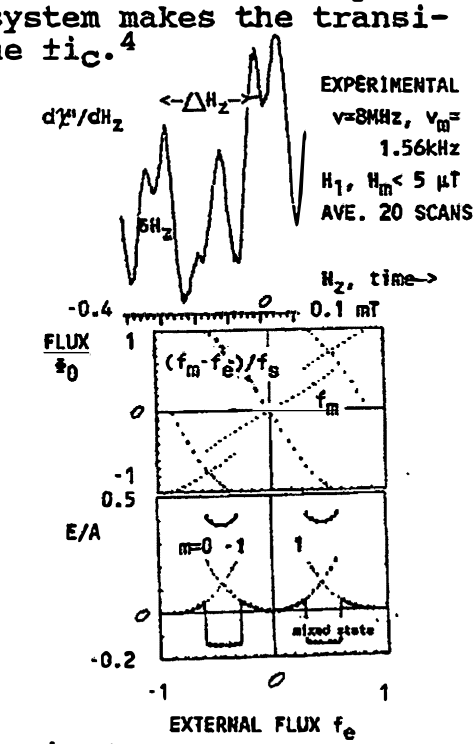

Fig.4 Experiment vs theory: $N=2$, $f_s=1/2\pi$

where $A=\pi\Phi_0 i_c(2\pi f_s/N + 1)/N$ and $|V/A| = N/(2\pi(2\pi f_s/N + 1)^{\frac{1}{2}})$ gives the interaction potential introduced by the Josephson junctions when a pair of free electrons moving in a ring in the state m are mixed with the states m±1 by the scattering potential V.[6] A discontinuous interaction with the oscillating field occurs when i(circ) reaches the value $\pm i_c$ then $\triangle m=\pm 1$ at $\pm(f_e - m)=\frac{1}{2}+f_s$ $=\frac{1}{2}+\frac{1}{2}\delta H_z/\triangle H_z=0.7$ in Fig. 4, **i.e.,** the fine structure consists of lines of opposite polarity when $(\pi/2 + 2\pi f_s/N) \geq \pi/N$ even if $2\pi f_s/N \ll 1$ when $N \geq 2$. The data in Fig. 4 obtain for N = 2, f_s = 0.2. Then within the accuracy of the measurement f_s is due to L_J alone, **i.e.,** $f_s = 1/2\pi$, and $A = 2.55 i_c\Phi_0$, $|V/A| \approx \sqrt{2}/\sqrt{3}/\pi$ and, Fig. 4 shows the data together E and $(f_m - f_e)$ vs f_e.

The heat capacity change can be deduced from Fig. 5 as $T \rightarrow T_c$. The slope of the T vs t, dT/dt decreases at the transition temperature indicating that C_p is diverging at that temperature.

5. Conclusions

The critical phenomena observed in the Meissner signal is similar to that observed for the thermopower,[7] and gives an accurate method for establishing T_c. The orientation dependence of the Meissner signal indicates that both H_1 and H_z determine the induced current which gives rise to the peiodic signal in Fig. 4. The differential calorimetry measurements confirm that the susceptibility diverges at T_c.

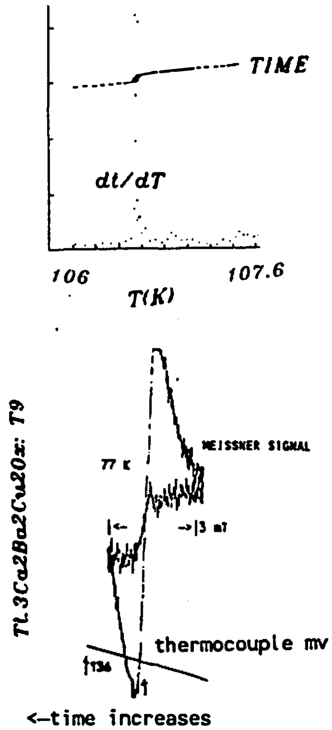

Fig.5 Signal enhancement near T_c
The slope of dT/dt->0 near 106 K.
a:Meissner signal. b:t, dt/dT vs T.

6. Acknowledgements

This work was carried out under the auspices of NSF grants DMR 8921163 and INT 8922483.

7. References

1. Acrivos, J. V.; Ithnin, R.; Bustillo, C.; Chen Lei, M.; and Hellmoldt, D., Physica C, **1990**, 162-164, 1665.

2. Wertz, J. E.; Koelsch, F. O.; Vivó,(Acrivos) J. J. Chem. Phys. **1955**, 23, 2194.

3. Schmid, A. Phys. Rev. **1969** 180 527.

4. a)Silver, A. H. and Zimmerman, J. E. Phys. Rev. **1967** 177 317; b)Blazey, K. W.; Portis, A. M. and Holtzberg, F. H. Physica C 1989 157, 16; c)Vichery, H.; Beuneu, F. and Lejay, P. Physica C **1989**, C159, 816; d)Jeffries, C. D.; Lam, Q. H.; Kim, Y.; Kim, C. M.; Zettl, A.; Klein, M. P. Phys Rev **1989**, B39, 11526.

5. Tinkham, M. **1975**, **"Introduction to Superconductivity"**, eq. (6.50).

6. Blatt, J. M. **"Theory of Superconductivity"**, **1964**, Acad. Press Ch VII, 6.

7. Howson, M.A.; Salamon, M.B.; Friedman, T.A.; Rice, J.P. and Ginsberg, D. Phys Rev **1990** B41, 300.